

This is an Open Access document downloaded from ORCA, Cardiff University's institutional repository:<https://orca.cardiff.ac.uk/id/eprint/177867/>

This is the author's version of a work that was submitted to / accepted for publication.

Citation for final published version:

Dong, Xiaohong, Ren, Yanqi, Zhou, Yue , Si, Qianyu, Dong, Xing and Wang, Mingshen 2025. Flexibility characterization and analysis of electric vehicle clusters based on real user behavior data. Applied Energy 387 , 125621. 10.1016/j.apenergy.2025.125621

Publishers page: <http://dx.doi.org/10.1016/j.apenergy.2025.125621>

Please note:

Changes made as a result of publishing processes such as copy-editing, formatting and page numbers may not be reflected in this version. For the definitive version of this publication, please refer to the published source. You are advised to consult the publisher's version if you wish to cite this paper.

This version is being made available in accordance with publisher policies. See <http://orca.cf.ac.uk/policies.html> for usage policies. Copyright and moral rights for publications made available in ORCA are retained by the copyright holders.



# Flexibility characterization and analysis of electric vehicle clusters based on real user behavior data

Xiaohong Dong<sup>a</sup>, Yanqi Ren<sup>a</sup>, Yue Zhou<sup>b</sup>, Qianyu Si<sup>a</sup>, Xing Dong<sup>a</sup>, Mingshen Wang<sup>c</sup>

<sup>a</sup> State Key Lab of Reliability and Intelligence of Electrical Equipment, Hebei University of Technology, Tianjin, 300130, China

<sup>b</sup> School of Engineering, Cardiff University, Cardiff CF24 3AA, Wales, UK

<sup>c</sup> State Grid Jiangsu Electric Power Research Institute, Nanjing 211103, China

**ABSTRACT:** With the increase in electric vehicles (EVs), they have begun to be valued as a new flexibility resource. Characterizing the flexibility of EVs is conducive to fully utilizing their flexibility to support the operation of electric power systems. A flexibility characterization method for EVs based on real user behavior data was proposed. First, the raw data are cleaned to obtain a dataset for each EV user. Then, a clustering algorithm is used to mine the plug-in time habit of each EV user, and an EV flexibility potential index system is proposed to quantify the flexibility of EV users with adjustable capacity, on-grid time, and charging power under the plug-in time habit. Furthermore, based on the flexibility indexes, the EV flexibility region under each plug-in time habit was constructed. Finally by setting the generators reasonably, the flexibility characterization from one EV user to the EV user cluster that includes large EVs is realized with the help of the zonotope similar. The flexibility of 6903 EV users in Nanjing, China, was characterized. The results showed that the similarity was improved by 0.566 by resetting the generator. Simultaneously, the results demonstrate the flexibility of the EV cluster in different periods. For example, there is a capacity adjustment range of approximately 75–150 MWh in 20:00-22:00, and approximately 15–20 MWh in 2:00-4:00 for the power grid to carry out day-ahead dispatching of EVs to assist the operation of the power grid.

**KEY WORDS:** Electric vehicles, Flexibility, User data, Zonotope, Flexible region

## NONMENCLATURE

### Abbreviations

EV	Electric Vehicle.
EVA	Electric Vehicles Aggregator.
SOC	State of Charge.

### Symbols

$\overline{Cap}_{in}^u$	The average plug-in battery capacity of the EV under data cluster $u$ .
$SOC_{in}^{i,u}$	The plug-in SOC value of the $i^{\text{th}}$ charging under data cluster $u$ .

$Cap_{max}$	The maximum battery capacity of the EV.
$N^u$	The total number of charging records under data cluster $u$ .
$Cap_{min}$	The minimum battery capacity of the EV
$SOC_{min}$	The minimum SOC value of the EV set by the user.
$SOC_{tra}^b$	The SOC value decreased caused by the $b^{\text{th}}$ trip.
$N_{tra}$	The total number of trip records
$Cap_{exp}^u$	The plug-out battery capacity EV users expect under data cluster $u$ .
$SOC_{out}^{i,u}$	The plug-out SOC value of the $i^{\text{th}}$ charging under data cluster $u$ .
$E_{\gamma}^{+,u}$	The upper boundary of the EV flexible region of $\gamma^{\text{th}}$ EV user under data cluster $u$ .
$E_{\gamma}^{-,u}$	The lower boundary of the EV flexible region of $\gamma^{\text{th}}$ EV user under data cluster $u$ .
$\overline{T}_{in}^u$	The average on-grid time of the EV under data cluster $u$ .
$t_{in}^{i,u}$	The on-grid time of the $i^{\text{th}}$ charging under data cluster $u$ .
$\overline{P}^u$	The average charging power of the EV under data cluster $u$ .
$P^i$	The charging power of the $i^{\text{th}}$ charging.
$P_d$	The discharging power of the EV.
$t_{end}^{c,min,u}$	The time when the battery is charged to the minimum battery capacity under data cluster $u$ .
$t_{end}^{c,max,u}$	The time when the battery is fully charged under data cluster $u$ .
$t_{end}^{d,u}$	The time when the battery is discharged to the minimum battery capacity under data cluster $u$ .
$t_{st}^u$	The time when charging is forced to start from the minimum battery capacity under data cluster $u$ .
$Cap_{out}^{c,u}$	The plug-out battery capacity after charging under data cluster $u$ .
$t_{out}^u$	The plug-out time under data cluster $u$ .
$t_{in,u}$	The plug-in time under data cluster $u$ .
$Cap_{out}^{d,u}$	The plug-out battery capacity after discharging under data cluster $u$ .
$F_{\gamma}^{z,u}$	The EV flexible region under data cluster $u$ of $\gamma^{\text{th}}$ EV user.
$c$	The center point of the zonotope.
$\mathbf{g}^{(k)}$	The $k^{\text{th}}$ generator vector of the zonotope.

$\beta_k$	The scaling coefficient of the $k^{\text{th}}$ generator vector.
$p$	The number of generator vectors.
$A_\gamma^u$	The coefficient matrix of the inequality from the EV flexible region boundaries under data cluster $u$ .
$b_\gamma^u$	The column vector of the inequality from the EV flexible region boundaries under data cluster $u$ .
$G^u$	The matrix of the generator vectors under data cluster $u$ .
$\beta_{\max}$	The maximum scaling coefficient vector.
$n_f$	The number of tangent planes of the zonotope.
$L_{z,h}$	The distance matrix for the various tangent planes of the zonotope.
$M$	The normal vector matrix of all the tangent planes of the zonotope.
$D_{F,h}$	The distance of the EV flexible region in the direction of the $h^{\text{th}}$ facet-normal

## 1 Introduction

Recently, an increasing number of renewable energy sources have been connected to the power grid, and the uncertainty caused by the large amount of renewable energy output has resulted in new impacts and challenges for the power grid. The flexibility provided by traditional thermal power units is gradually being unable to meet the flexibility demands of new power system characterized by dealing with the variability and uncertainty of power generation and load<sup>[1]</sup>. According to the International Energy Agency<sup>[2]</sup>, the global Electric Vehicle (EV) stock is growing rapidly, and EV sales worldwide were 13.8 million in 2023, increasing by approximately 35 % over the previous year. The global EV stock reached 40 million.

As a special load, a large number of EVs are connected to the power grid, which may intensify the load peak-valley difference, increase network loss, and increase the frequency fluctuation of the power grid. Simultaneously, EVs have great potential as a flexible resource. A reasonable characterization of the flexibility potential will be conducive to vehicle-grid interaction and the optimization of power grid operation.

EV flexibility refers to the ability of EVs to adjust their loads through charging and discharging control<sup>[3]</sup>. Through reasonable electricity price guidance, the EV charging load can be effectively utilized to improve the flexibility of the power system<sup>[4]</sup>, while reducing carbon dioxide emissions<sup>[6]</sup> and the unbalanced risk of the power grid owing to renewable energy connections<sup>[7]</sup>. A multi-objective optimization model considering organizational expenditures and battery degradation costs was developed in<sup>[8]</sup>, enabling electric vehicles to participate in industrial smart grids to enhance operational flexibility. The charging and discharging behavior of electric vehicles is optimized in<sup>[9]</sup>, which utilizes electric vehicles as a component of the home energy management system, thereby reducing the

energy consumption and cost of the residence. The potential of electric vehicles (EVs) in Germany to mitigate load demand fluctuations is examined in<sup>[10]</sup>, which elucidates the inherent conflict between national and regional incentive mechanisms. The above research utilizes EV flexibility to effectively optimize the operation of power systems, but EV flexibility models are relatively simple and cannot characterize the behavior habits of users. The accurate characterization of EV flexibility considering the behavioral habits of users is still an urgent problem that needs to be solved.

Several scholars have investigated this issue. Various EV charging and discharging models have been established to characterize the energy and power flexibility boundaries of EVs in<sup>[11]</sup>. EV flexibility was transformed into the demand response capability, which realizes the quantification of EV flexibility in<sup>[12]</sup>. Based on the EV charging load results by Monte Carlo simulations, the ability of EV flexibility to consume photovoltaic power generation was quantified in<sup>[14]</sup>. The deviation value of the SOC was added to the SOC curve during EV charging, and the flexibility of the EV in the charging process was evaluated to minimize the operating cost caused by the deviation value in<sup>[16]</sup>. The definition of flexibility for a charging station was explored, and a charging strategy of the charging station for maximizing flexibility was proposed in<sup>[17]</sup>. EV flexibility under different charging power and electricity price scenarios was studied in<sup>[18]</sup>, and the flexibility of different EV types was quantified. However, the existing EV flexibility models rely on simulations. Setting scenarios in advance to simulate the behavior of EV users cannot truly represent the behavior habits of EV users, and thus cannot truly characterize the flexibility potential of EVs.

Therefore, some scholars have characterized EV flexibility by analyzing real EV user data. An algorithm for mining EV flexibility was proposed, and its flexibility was evaluated by calculating an index using a data-driven algorithm<sup>[19]</sup>. The EV charging data were analyzed, and the EV flexibility in capacity and time was characterized by converting the EV flexibility into the demand response capability in<sup>[20]</sup>. The types of EV charging behavior in the dataset were identified. By analyzing the characteristics of different charging behaviors and combining multi-source data such as weather, EV flexibility in each period of the day was quantified in<sup>[22]</sup>. However, the above research based on EV charging data does not consider the behavior habits of EV users. At the same time, the research results are in a single form, and a simple value cannot reflect the boundary of EV charging and discharging dispatching when EV was plugged-in. Moreover, the above research only quantified the flexibility of a single EV user; however, when a large number of EVs are

connected to the power grid, it causes great pressure on the power grid. Moreover, EVs have far greater dispatching potential than a single EV; therefore, it is necessary to study the flexibility of EVs.

To address these problems, scholars have conducted further research on the flexibility of EVs. An evaluation method for the upward and downward flexibility of EV was proposed and the flexibility of EVs was studied under different dispatching strategies in [23]. A market framework based on the Electric Vehicle Aggregator (EVA) was proposed in [25], which directly analyzed and quantified the flexibility of the EVA. The EV flexibility was represented as the form of an EV flexible region in [26], which constructs the boundary of the EV participating in charging and discharging. The Minkowski sum was used to aggregate a large number of EV flexible regions, which enabled flexible characterization of EVs. An inner approximation method for flexible regions was proposed for flexible resources in [28]. The aggregation of the EV flexible region was realized by approximating the original EV flexible region to a specific polytope. A method for aggregating demand response resources was proposed in [30], which realized the rapid aggregation of many demand response resources by using the characteristics of the polytope. An aggregation method for distributed energy resources based on the zonotope was proposed in [31]; however, this method was not well adapted to the EV flexible region.

In general, most existing methods are based on simulation data, which are unreliable in practical applications. Among the data-driven methods, the aggregation method based on the Minkowski sum has low computational efficiency and cannot complete the aggregation of flexible areas of large-scale EVs. The polytope-based method cannot be directly applied to an EV flexible region. Therefore, a new look is brought to the existing methods in the following areas: (I) EV flexibility modeling and (II) EV flexibility aggregation. The main contributions are summarized as follows:

1) Based on a real dataset, an EV flexibility potential index system was proposed, and the EV flexible region was constructed for a single EV user. Considering the behavior habits of users, the flexibility of a single EV user is characterized in the form of EV flexible region, which solves the problem that the existing flexibility characterization methods have less respect for the behavior habits of users.

2) Because the existing aggregation method based on the Minkowski sum is computationally inefficient, generators are redesigned based on [31] to make the aggregation model more adaptable to EV flexible regions, complete EV flexible region approximation at the cost of minimum flexibility loss, and realize EV flexible region aggregation.

3) The high computational efficiency achieved using the zonotope approximation of the EV flexible region promotes the aggregation of the flexible region of large-scale EVs. It effectively solves the problem of the insufficient support capacity of a single EV and captures the flexible characteristics of EVs.

The organizational structure of the remaining manuscript is as follows: The overview of the flexibility characterization of EVs based on real user behavior data is described in the second section. The construction method of flexible region of a single EV user is detailed explained in the third section. The EV flexible region approximation model based on the zonotope is introduced in the fourth section. The EV flexible region aggregation model is described in the fifth section. The example and results are analyzed in the sixth section. The conclusion and future study are summarized in the seventh section.

## 2 The overview of the proposed method

The proposed method was used to characterize the flexibility of EVs in a bottom-up manner, as shown in Fig.1. The proposed method is mainly composed of the flexible region construction of a single EV user, flexible region approximation of a single EV user, and EV flexible region aggregation for constructing the flexible region of EV cluster. The details are presented below.

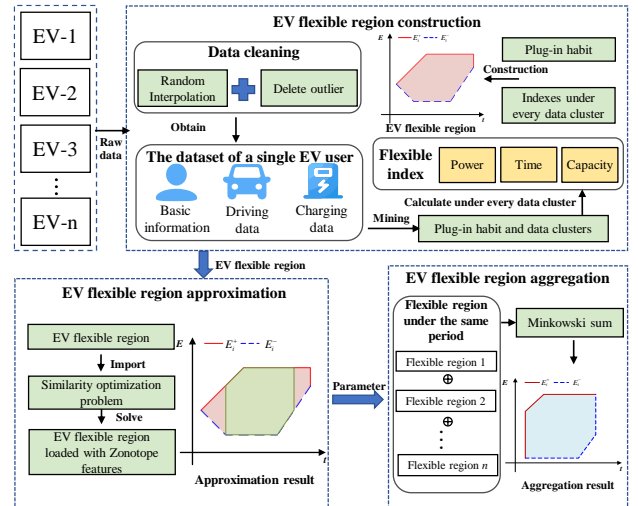


Fig. 1 The overview of the proposed method

1) Flexible region construction of a single EV user: The real behavior data of EV users are analyzed, and a single EV user dataset is obtained. Subsequently, an EV flexibility potential index system was built based on a single EV user dataset. Finally, the EV flexible region of a single EV user considering plug-in time habits was constructed by combining the EV flexibility potential index system based on real behavior data.

2) Flexible region approximation of a single EV user: By setting reasonable generators, the optimization problem with the goal of maximizing similarity is

solved, and the flexible region of a single EV user is approximated by zonotope.

3) EV flexible region aggregation: With the high aggregation efficiency of the zonotope, the Minkowski sum is applied to the flexible region of a single EV user after approximating the same interval. Many EV flexible regions were aggregated to characterize the flexibility of EVs. The result is the flexibility of EVs for a day.

### 3 Flexible region construction based on real behavior data of EV users

First, the raw data must be cleaned to obtain the dataset for a single EV user. Then, a single EV user habit of plug-in time is mined, and an EV flexibility potential index system is proposed to calculate the flexibility indexes in terms of the adjustable capacity, on-grid time, and charging power under every plug-in time for a single EV. Finally, the flexible region of a single EV user was constructed by calculating the upper and lower boundaries based on the flexibility indexes.

#### 3.1 The dataset of a single EV user

The raw dataset contains basic information, charging data, and traveling data of EV users, as shown in Tab.1. The basic information includes user ID, vehicle type, and nominal battery capacity. The charging data included the start and end times of charging, charging power, plug-in SOC value, and plug-out SOC value. The traveling data included the SOC value decreased caused by the trip. Because of errors during data acquisition, communication failures, etc., there is a lot of unavailable raw data. Thus, data preprocessing of raw datasets is necessary. Data preprocessing included the processing of outliers and missing values, data merging, and reconstruction.

The outliers were filtered based on the data distribution. The random interpolation method was used to randomly fill in missing data based on the data distribution. Specifically, outliers included charging power higher than 350 kW or lower than 3 kW, charging time of less than 5 min, plug-in SOC value of less than 3 %, and traveling time of less than 5 min. These outliers were deleted. After preprocessing, each EV user obtains the dataset shown in Tab.1, which contains the basic information, charging, and travel records of the EV user.

#### 3.2 EV flexibility potential index system

Each EV user may exhibit multiple charging behaviors with different flexibilities. First, based on the dataset of single EV user data in Section 3.1, the plug-in time of a single EV user was clustered in combination with the historical charging behavior. The plug-in time habits of the EV users were obtained, and the dataset of a single EV user was divided into

multiple clusters.

The EV flexibility potential index for every data cluster is built to depict when the EV user is used to plug-in and the flexibility after plug-in. The flexibility of power system resources necessitates careful consideration of their response time, respond capacity, and duration as shown in Fig.2. The index system is divided into three parts: adjustable capacity, on-grid time, and charging power, which characterize the flexibility potential of the EV for under data cluster  $u$ .

Tab.1 The dataset of a single EV user

Data type	Data name	Note
Basic information	User ID	For identifying users.
	Vehicle type	Private cars, Bus, Taxi, Official cars, Rental cars.
	$Cap_{max}$	Maximum battery capacity. (kWh)
	Plug-in time / Plug-out time /	
Charging data	$SOC_{in}^i$	The plug-in SOC value of the $i^{\text{th}}$ charging.
	$SOC_{out}^i$	The plug-out SOC value of the $i^{\text{th}}$ charging.
	$P^i$	The charging power of the $i^{\text{th}}$ charging record (kW).
Driving data	$SOC_{tra}^b$	The SOC value decreased caused by the $b^{\text{th}}$ trip (kWh).

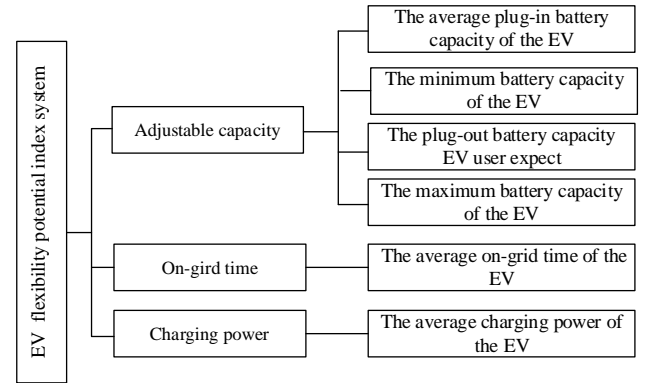


Fig. 2 The EV flexibility potential index system

The average plug-in battery capacity  $\overline{Cap}_{in}^u$  of the single EV under data cluster  $u$  is calculated by the equation (1).

$$\overline{Cap}_{in}^u = \frac{\sum_{i=1}^{N_u} SOC_{in}^{i,u}}{N_u} Cap_{max} \quad (1)$$

where  $SOC_{in}^{i,u}$  is the plug-in SOC value of the  $i^{\text{th}}$  charging under data cluster  $u$  for the single EV;  $Cap_{max}$  is the maximum battery capacity of the EV and represents the upper limit battery capacity of the EV. This value is fixed in any data cluster;  $N_u$  is the total number of charging records under data cluster  $u$  for the

single EV.

The minimum battery capacity  $Cap_{\min}$  of the EV which meets lowest traveling demand of users, is calculated by the equation (2).

$$Cap_{\min} = (1 - SOC_{\min} + \frac{\sum_{b=1}^{N_{tra}} SOC_{tra}^b}{N_{tra}}) Cap_{\max} \quad (2)$$

where  $SOC_{\min}$  is the minimum SOC value set to protect the health of battery;  $SOC_{tra}^b$  is the SOC value decreased caused by the  $b^{\text{th}}$  trip;  $N_{tra}$  is the total number of trips.

The plug-out capacity the EV user expects  $Cap_{\exp}^u$  under data cluster  $u$  is depicted by the equation (3).

$$Cap_{\exp}^u = Cap_{\min} + \frac{\sum_{i=1}^{N_u} SOC_{out}^{i,u}}{N_u} Cap_{\max} \quad (3)$$

where  $SOC_{out}^{i,u}$  is the plug-out SOC value of the  $i^{\text{th}}$  charging under data cluster  $u$ .

The average on-grid time  $\bar{T}_{in}^u$  of the EV under data cluster  $u$  is calculated by the equation (4).

$$\bar{T}_{in}^u = \sum_{i=1}^{N_u} t_{in}^{i,u} / N_u \quad (4)$$

where  $t_{in}^{i,u}$  is the on-grid time of the  $i^{\text{th}}$  charging record under data cluster  $u$  for the single EV user.

The average charging power  $\bar{P}^u$  of the EV under data cluster  $u$  is calculated by the equation (5).

$$\bar{P}^u = \sum_{i=1}^{N_u} P^{i,u} / N_u \quad (5)$$

where  $P^{i,u}$  is the charging power of the  $i^{\text{th}}$  charging record under data cluster  $u$ ,  $\bar{P}^u$  means that EV users may have different charging power limits at different plug-in time.

### 3.3 Flexible region construction of a single EV user

Based on the EV flexibility potential indexes of each cluster for a single EV user, EV flexible regions were constructed. From Section 3.2, it can be seen that each EV user has different flexibility potential indexes under different plug-in time, that is, under different data clusters, which also means that the flexibility is not the same. For ease of description, we describe how to build a flexible region, although the flexibility of EV users is represented by multiple flexible regions.

Fig.3 shows an example of an EV flexible region. The EV flexible region indicates that the EV can charge and discharge in this region. The slopes of the upper and lower boundary edges of the flexible region correspond to the charging and discharging powers. When the slope is zero, the charge and discharge

powers are zero during this period. The number, location and shape of EV flexible regions for each EV user represent the flexibility distribution and size.

The flexible region consists of the upper boundary  $E_{\gamma}^{+,u}$  and the lower boundary  $E_{\gamma}^{-,u}$  for the  $\gamma^{\text{th}}$  EV under data cluster  $u$ . In this example, the upper boundary  $E_{\gamma}^{+,u}$  indicates that the EV is charged to maximum battery capacity immediately after plugging-in, then stops charging, and finally plug-out. The lower boundary  $E_{\gamma}^{-,u}$  indicates that the EV is discharged to the minimum battery capacity before being charged, then stops discharging, and finally plug-out after a period of forced charging.  $\bar{Cap}_{in}^u$ ,  $Cap_{\max}$ ,  $Cap_{\exp}^u$ , and  $Cap_{\min}^u$  can be obtained directly from the index system.  $t_{end}^{c,max,u}$ ,  $t_{end}^{d,u}$ ,  $t_{st}^u$ , and  $t_{out}^u$  can be determined by the equations (6)-(9) based on the values of the EV flexibility potential indexes under data cluster  $u$ .

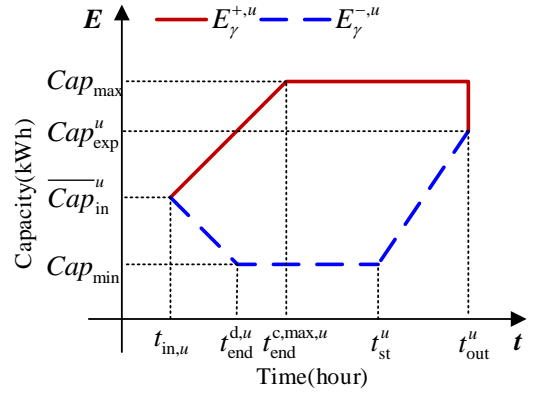


Fig. 3 An example of the EV flexible region

$$t_{end}^{c,max,u} = t_{in,u} + (Cap_{\max} - \bar{Cap}_{in}^u) / \bar{P}^u \quad (6)$$

$$t_{end}^{d,u} = t_{in,u} + (\bar{Cap}_{in}^u - Cap_{\min}) / P_d \quad (7)$$

$$t_{st}^u = t_{in,u} + \bar{T}_{in}^u - (Cap_{\exp}^u - Cap_{\min}) / \bar{P}^u \quad (8)$$

$$t_{out}^u = t_{in,u} + \bar{T}_{in}^u \quad (9)$$

where  $t_{end}^{c,max,u}$  is the time when the battery is charged to the maximum battery capacity of the EV under data cluster  $u$ ;  $t_{in,u}$  is the cluster center of the plug-in time under data cluster  $u$ , which represents the plug-in time habit EV users;  $t_{end}^{d,u}$  is the time when the battery is discharged to  $Cap_{\min}$  under data cluster  $u$ ;  $P_d$  is the discharging power;  $t_{st}^u$  is the time when the EV is forced to start charging from  $Cap_{\min}$  under data cluster  $u$ ;  $t_{out}^u$  is the off-grid time under data cluster  $u$ .

The above variables in (6)-(9) combined with the EV flexibility potential index together constitute the upper and lower boundaries of the EV flexible region. Owing to the limitations of charging power, on-grid time, and plug-in capacity, the above variables will be different, which will lead to different shapes of the EV

flexible regions. By analyzing the relationships among the variables in (6)-(9), some points at the upper and lower boundaries are calculated and connected to obtain the EV flexible regions.

The upper boundary can be calculated by (10). If the off-grid time  $t_{out}^u$  is later than or equal to the time when the battery is fully charged  $t_{end}^{c,max,u}$ , the EV can be charged to the maximum battery capacity of the EV before the off-grid time  $t_{out}^u$ . In this case, the upper boundary will be the line A in Fig.4. Otherwise, if  $t_{out}^u$  is sooner than  $t_{end}^{c,max,u}$ , the upper boundary will be the line B in Fig.4.

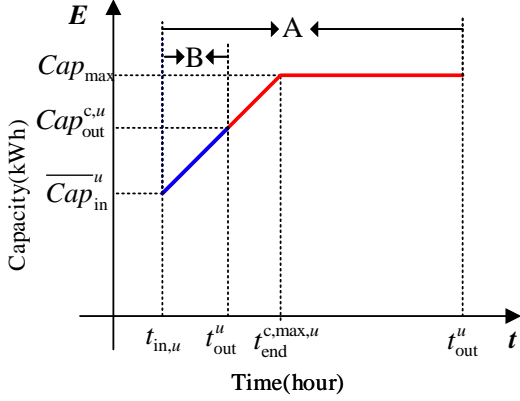


Fig. 4 The upper boundary construction diagram

upper boundary points=

$$\begin{cases} (t_{in,u}, \overline{Cap}_{in}^u), (t_{end}^{c,max,u}, Cap_{max}), (t_{out}^u, Cap_{max}) & t_{out}^u \geq t_{end}^{c,max,u} \\ (t_{in,u}, \overline{Cap}_{in}^u), (t_{out}^u, Cap_{out}^{c,u}) & t_{out}^u < t_{end}^{c,max,u} \end{cases} \quad (10)$$

where,  $Cap_{out}^{c,u}$  is the plug-out battery capacity after charging, and determined by the equation (11).

$$Cap_{out}^{c,u} = \overline{Cap}_{in}^u + (t_{out}^u - t_{in,u}) \overline{P}^u \quad (11)$$

To calculate the lower boundary, two scenarios need to be considered: Scenario I – the EV discharging immediately after plugging-in; Scenario II – the EV charging first before discharging after plugging-in. In Scenario I, the average plug-in battery capacity under data cluster  $u$   $\overline{Cap}_{in}^u$  is larger than the minimum battery capacity of the EV  $Cap_{min}$ , and the lower boundary can be calculated by the equation (12).

lower boundary points of the Scenario I =

$$\begin{cases} (t_{in,u}, \overline{Cap}_{in}^u), (t_{end}^{d,u}, Cap_{min}), & t_{end}^{d,u} \leq t_{st}^u \\ (t_{st}^u, Cap_{min}), (t_{out}^u, Cap_{exp}^u) \\ (t_{in,u}, \overline{Cap}_{in}^u), (t_{end}^{d,u}, Cap_{end}^{d,u}), & t_{st}^u < t_{end}^{d,u} \leq t_{out}^u \\ (t_{out}^u, Cap_{exp}^u) \\ (t_{in,u}, \overline{Cap}_{in}^u), (t_{out}^u, Cap_{end}^{d,u}) & t_{out}^u < t_{end}^{d,u} \end{cases} \quad (12)$$

where  $Cap_{end}^{d,u}$  is the plug-out battery capacity after

discharging under data cluster  $u$  determined by (13).

$$Cap_{end}^{d,u} = \overline{Cap}_{in}^u - P_d(t_{out}^u - t_{in,u}) \quad (13)$$

Based on (12), if the time  $t_{end}^{d,u}$  when the battery is discharged to  $Cap_{min}$  under data cluster  $u$  is sooner than or equal to the time  $t_{st}^u$  when the EV is forced to start charging from  $Cap_{min}$  under data cluster  $u$ , the EV can discharge to  $Cap_{min}$  before the plug-out time  $t_{out}^u$  under data cluster  $u$ , and then charge from  $Cap_{min}$  to  $Cap_{exp}^u$ . As a result, the lower boundary is the line A shown in Fig.5.

By contrast, if  $t_{end}^{d,u}$  is later than  $t_{st}^u$  but sooner than or equal to the plug-out time  $t_{out}^u$ , the EV starts charging immediately after the discharging process. The EV needs to be charged to  $Cap_{exp}^u$  after discharging. In this case, the lower boundary is shown as the line B in Fig. 5. If  $t_{end}^{d,u}$  is later than  $t_{out}^u$ , the lower boundary is shown in the line C of Fig.5.

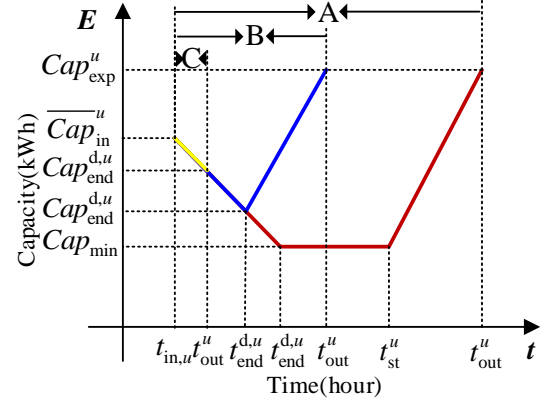


Fig. 5 The lower boundary of Scenario I

In Scenario II, the average plug-in battery capacity  $\overline{Cap}_{in}^u$  under data cluster  $u$  is smaller than  $Cap_{min}$ . That means the EV is immediately charged after plugging-in. The lower boundary of the Scenario II can be calculated by the equation (14).

lower boundary points of the Scenario II =

$$\begin{cases} (t_{in,u}, \overline{Cap}_{in}^u), (t_{end}^{c,min,u}, Cap_{min}), & t_{end}^{c,min,u} \leq t_{st}^u \\ (t_{st}^u, Cap_{min}), (t_{out}^u, Cap_{exp}^u) \\ (t_{in,u}, \overline{Cap}_{in}^u), (t_{end}^{c,min,u}, Cap_{min}^u), & t_{end}^{c,min,u} > t_{st}^u \\ (t_{out}^u, Cap_{min}) \end{cases} \quad (14)$$

where  $t_{end}^{c,min,u}$  is the time when the battery is charged to  $Cap_{min}$  under data cluster  $u$  and determined by the equation (15).

$$t_{end}^{c,min,u} = t_{in,u} + (Cap_{min} - \overline{Cap}_{in}^u) / \overline{P}^u \quad (15)$$

According to (14), if the time when the battery is charged to the minimum battery capacity  $t_{end}^{c,min,u}$  under data cluster  $u$  is sooner than or equal to the time  $t_{st}^u$

when the EV is forced to start charging from the minimum battery capacity of the EV under data cluster  $u$ , the EV can be charged to the plug-out battery capacity  $Cap_{exp}^u$ . EV user expect under data cluster  $u$  before the plug-out time  $t_{out}^u$ . Then the lower boundary is shown as the line A in Fig. 6. Otherwise, when  $t_{end}^{c, min, u}$  is later than  $t_{st}^u$ , the lower boundary is shown as the line B in Fig.6.

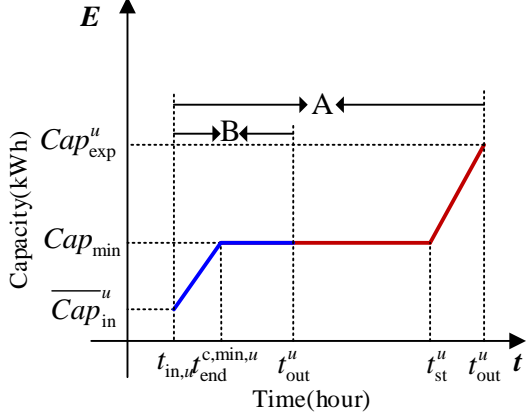


Fig. 6 The lower boundary of Scenario II

## 4 EV flexible region approximation

To construct the flexible region from large numbers of one EV user to the EV user cluster, the zonotope theory is used to approximate the flexible region of a single EV user to reduce the computational burden for aggregating regions later.

### 4.1 Overview of the zonotope theory

Zonotope is a special geometric convex polytope with central symmetry. It is flexible and can change its shape and size by adjusting the number and direction of generator vectors<sup>[32]</sup>. The zonotope can be expressed as a center point and multiple generator vectors, as shown in (16). By reasonably selecting the number of generator vectors and size of the scaling coefficient, any zonotope can be generated. Zonotope can also be represented in abstract form, as shown in (17), featuring three parameters: the center point, generator vectors, and scaling coefficients.

$$Z = \{z \in \mathbb{R}^n \mid z = c + \sum_{k=1}^p \beta_k \mathbf{g}^{(k)}, \beta_{\min} \leq \beta_k \leq \beta_{\max}\} \quad (16)$$

$$Z = Z(c, \mathbf{g}^{(1)} \beta^{(1)}, \dots, \mathbf{g}^{(p)} \beta^{(p)}) \quad (17)$$

where  $n$  is the dimension of zonotope;  $c$  is the center point of the zonotope;  $\mathbf{g}^{(k)}$  represents the  $k^{\text{th}}$  generator vector, which determines the direction of the zonotope extends from the center point;  $\beta_k$  is the scaling coefficient of the  $k^{\text{th}}$  generator vector, which determines the distance of the generator vector from the center point to the boundary of the zonotope;  $p$  represents the number of generator vectors.

### 4.2 The approximation method

Because the shape of the zonotope can be flexibly changed by adjusting the parameters, it can be easily aggregated. An approximation method is introduced for describing flexible region of a single EV user using zonotope.

The approximation is realized by solving an approximation optimization problem. The objective function of this optimization problem is to maximize the similarity between the zonotope and the original EV flexible region, with the constraint that the zonotope is contained in the original EV flexible region. The approximation optimization model was constructed as follows:

First, the EV flexible region constructed in Section 3.3 is transformed into a half-plane representation of polytope<sup>[33]</sup>, as shown in (18).

$$F_\gamma^u = \{f_\gamma^u \in \mathbb{R}^n \mid \mathbf{A}_\gamma^u f_\gamma^u \leq \mathbf{b}_\gamma^u\} \quad (18)$$

where  $F_\gamma^u$  is the EV flexible region under data cluster  $u$  of the  $\gamma^{\text{th}}$  EV user;  $f_\gamma^u$  is the feasible point set within the EV flexible region;  $\mathbf{A}_\gamma^u$  and  $\mathbf{b}_\gamma^u$  are the coefficient matrix and constant column vectors of the inequality for representing the edges of the EV flexible region under data cluster  $u$  of the  $\gamma^{\text{th}}$  EV user.

To guarantee that the constructed zonotope is contained in the original EV flexible region, (19) is derived based on (16) and (18):

$$\mathbf{A}_\gamma^u (c + \sum_{k=1}^p \beta_k \mathbf{g}^{(k)}) \leq \mathbf{b}_\gamma^u, \beta_{\min} \leq \beta_k \leq \beta_{\max} \quad (19)$$

to simplify the representation, the scaling method is also used. The generators and the scaling coefficient are summarized in matrix form, thus obtaining (20).

$$\mathbf{A}_\gamma^u c + \left| \mathbf{A}_\gamma^u \mathbf{G}^u \right| \boldsymbol{\beta}_{\max} \leq \mathbf{b}_\gamma^u \quad (20)$$

where  $|\cdot|$  denotes to take the absolute value for each element of the matrix;  $c$  is the center point of the approximate zonotope;  $\boldsymbol{\beta}_{\max}$  is the maximum scaling coefficient vector.

In equation (20),  $\mathbf{G}^u$  is the generator vector matrix of the zonotope for the EV flexible region under data cluster  $u$  of the  $\gamma^{\text{th}}$  EV user, but the generator vector provided in [31] cannot adapt well to the characteristics of the EV flexible region. Therefore, the generator vector matrix is proposed, as shown in (21).

$$\mathbf{G}^u = \begin{bmatrix} 1 & 0 & 1/\sqrt{(\overline{P}^u)^2 + 1} & -1/\sqrt{P_d^2 + 1} \\ 0 & 1 & (\overline{P}^u)^2 / \sqrt{(\overline{P}^u)^2 + 1} & P_d / \sqrt{P_d^2 + 1} \end{bmatrix} \quad (21)$$

next, the objective function of the approximation optimization model is to maximize similarity  $\Delta_z$  equaling to the average of the proportion of the distance between each parallel facet of zonotope and the

distance of each direction of polytope facet-normal for the EV flexible region, as shown in Fig.7 and the equation (22).

$$\max \Delta_Z = \frac{1}{n_f} \sum_{h=1}^{n_f} \frac{L_{z,h}}{\mathbf{D}_{F,h}} \quad (22)$$

where  $n_f$  is the number of pairs of parallel facets of the zonotope;  $L_{z,h}$  is the distance between  $h^{\text{th}}$  pair of parallel facets of zonotope;  $\mathbf{D}_{F,h}$  is the distance of the EV flexible region in the direction of the  $h^{\text{th}}$  facet-normal;  $L_{z,h}$  is formed into matrix  $\mathbf{L}_{z,h} = 2|\mathbf{M}^\top \mathbf{G}^u| \boldsymbol{\beta}_{\max}$ ;  $\mathbf{M} = [m^1, \dots, m^{n_f}]^\top \in \mathbb{R}^{n \times n_f}$  is the normal matrix, which contains the normal vectors of all possible facets of the zonotope,  $\mathbf{D}_{F,h}$  is formed into vector set  $\mathbf{D}_{F,h} = [D_1, \dots, D_{n_f}]^\top$ .

The zonotope approximates the EV flexible region perfectly only if  $L_{z,h} = \mathbf{D}_{F,h}$ . Combining the objective function and constraints, the approximation optimization model is formulated as a linear programming problem. The decision variables for this problem are  $c$  and  $\boldsymbol{\beta}_{\max}$ . The formulation is as below:

$$\max_{\{c, \boldsymbol{\beta}_{\max}\}} \frac{2}{n_f} (\mathbf{1} / \mathbf{D}_{F,h})^\top |\mathbf{M}^\top \mathbf{G}^u|^\top \boldsymbol{\beta}_{\max} \quad (23)$$

$$\text{s.t. } \mathbf{A}_\gamma^u c + |\mathbf{A}_\gamma^u \mathbf{G}^u| \boldsymbol{\beta}_{\max} \leq \mathbf{b} \quad (24)$$

$$\boldsymbol{\beta}_{\max} \geq 0 \quad (25)$$

where  $/$  is the division of matrix elements

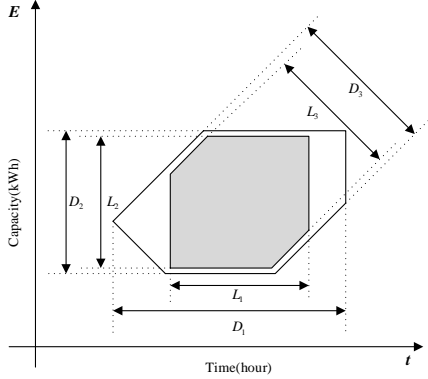


Fig. 6 The diagram of the Zonotope approximation calculation

## 5 EV flexible region aggregation

The aggregation of multiple EV flexible regions is realized by calculating the Minkowski sum of them to characterize the flexibility of the EVs. Firstly, the scaling coefficient vector  $\boldsymbol{\beta}_{\max}$  and center point  $c$  will be solved by the optimization model. The optimal approximation form  $F_\gamma^{z,u}$  of zonotope for the EV flexible region under data cluster  $u$  of  $\gamma^{\text{th}}$  EV user is obtained as (26).

$$F_\gamma^{z,u} = Z(c_\gamma, \mathbf{g}_\gamma^{(1)} \beta_\gamma^{(1)}, \dots, \mathbf{g}_\gamma^{(p)} \beta_\gamma^{(p)}) \quad (26)$$

where  $c_\gamma$  is the center point of the approximate zonotope,  $\mathbf{g}_\gamma$  is the generator vector from generator vector matrix  $\mathbf{G}^u$ , and  $\beta_\gamma$  is the scaling coefficient from the scaling coefficient vector  $\boldsymbol{\beta}_{\max}$ .

Then it is ready to calculate the Minkowski sum of the EV flexible regions in the same period, denoted as  $\oplus$ . The aggregation of any two EV flexible regions  $\sigma$  and  $\eta$  is shown in (27). The aggregated EV flexible region can be guaranteed to be a convex set and contain all feasible points. The flexibility characterization of EVs is realized by this.

$$F_\sigma^{z,u} \oplus F_\eta^{z,u} = Z(c_\sigma + c_\eta, \mathbf{g}_\sigma^{(1)} \beta_\eta^{(1)}, \dots, \mathbf{g}_\sigma^{(p)} \beta_\eta^{(p)}, \mathbf{g}_\sigma^{(1)} \beta_\eta^{(1)}, \dots, \mathbf{g}_\sigma^{(q)} \beta_\eta^{(q)}) \quad (27)$$

## 6 Result and analysis

The data used are from the real behavior data of 6903 electric vehicle users in Nanjing, China, from May 2021 to May 2022. As introduced in Section 3.1, it includes basic information, charging data, and driving data. The data set includes 1,400 taxis, 2,990 private cars, 1,784 rental cars, 439 official cars, and 290 buses. The total number of data entries is nearly 1.4 million.

### 6.1 EV flexible region type analysis

Through the construction of the EV flexible region, 20160 EV flexible regions are constructed for 6903 EV users. From the perspective of types of flexible regions, they can be divided into seven categories. By analyzing the type of flexible region, the charging habits of different vehicles can be obtained, such as several times of plug-in in a day, when to plug-in, and flexibility after plug-in. In order to better illustrate the characteristics of different EV flexible regions, this study selects an example for each type of EV flexible region, as shown in Fig.8. Some capacity variables related to the EV flexible region are shown in Fig.8.

It can be seen that the plug-in capacity of (a), (b), (c), and (d), the four types of EV flexible regions are higher than the minimum capacity and can participate in the discharge immediately after plugging-in, while the three types of (e), (f), and (g). The class (a) EV flexible region conforms to the ideal state, and its upper and lower boundaries are line A under Scenario I of Section 3.3, which is due to its long on-grid time and large charging power. As the flexibility potential index changes, the EV flexibility region will change, such as (b) (c) (d), and their flexibility is less than (a). In contrast to the (a) type, the lower boundary of the (g) type is line A under Scenario II of Section 3.3, which is because its plug-in capacity is lower than the minimum capacity.

To better illustrate the construction of the EV

flexible region, Fig.9 shows the EV flexible region of a private car user. It is found that the plug-in time of the private car user is relatively scattered and accustomed to charging at 0:00, 12:00, and around 22:00. These EV flexible regions belong to (a), (c), and (a) in Fig. 8, respectively, and their plug-in battery capacity is higher than the minimum battery capacity. The user can participate in discharging immediately after plugging-

in. However, the on-grid charging time at 12:00 h is relatively short. The other two flexible regions have a low plug-in capacity, which proves that the user used to charge after a day of work has a longer on-grid time. The flexible region construction result represents the characteristics of typical private car users, that is, charging for the short term at daytime and charging for the long term at night after returning home.

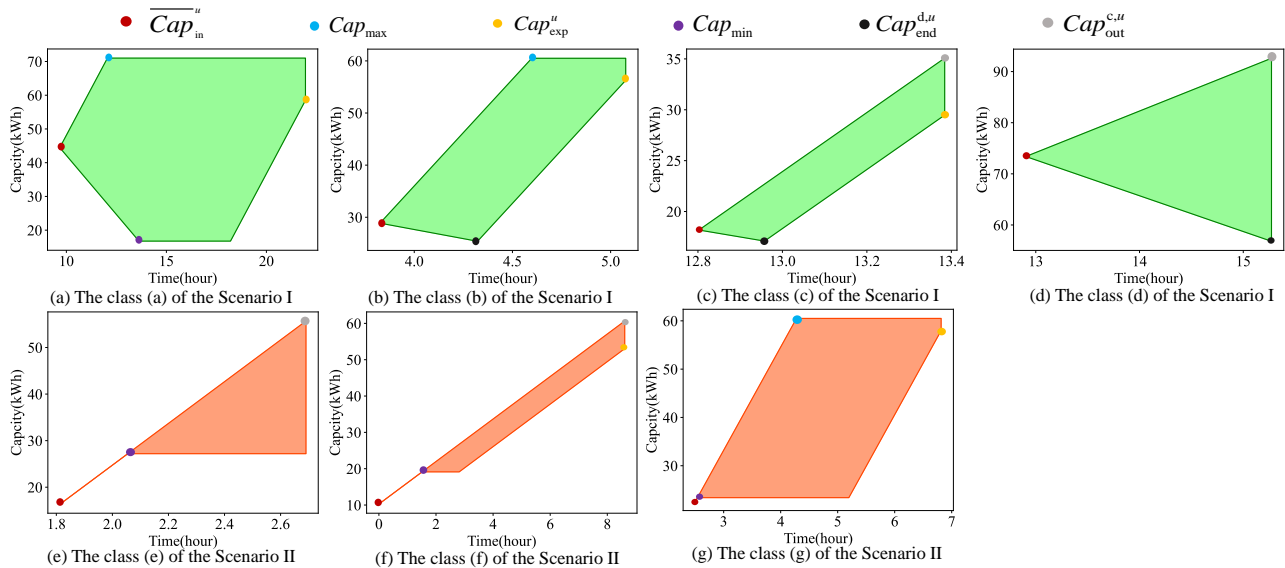


Fig. 8 The EV flexible region classes

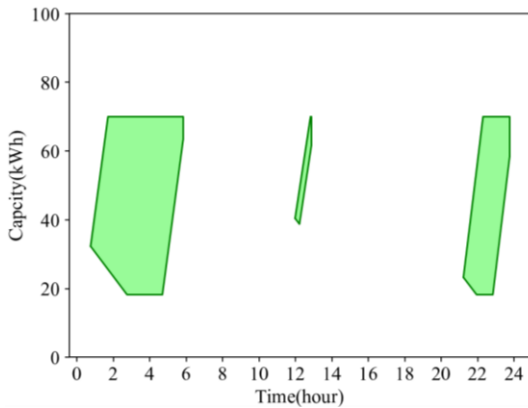


Fig. 9 The flexible region of a private car user

## 6.2 Flexible region analysis of EV application clusters

The aggregation of the flexible regions of different EV application clusters is carried out to discuss the flexibility differences, so that different guidance methods can be used for different EV applications in the future study, as shown in Fig.10. Taking 2 hours as the length of an interval, the 24-hour period is divided into 12 periods, and the flexible regions of a large number of EV users are aggregated in every time period.

The flexible region of the private car cluster is the largest, providing the greatest flexibility. The flexibility is quite dispersed. Most of the flexibility is concentrated in the period from 10:00 to 22:00, and the capacity adjustment range varies from 20 MWh to 80 MWh. Most of them are accustomed to slow charging at home, and the overall load level is low, more suitable to participate in the capacity market.

In contrast, taxi, and rental car are commercial vehicles and are often accustomed to fast charging. Therefore, they have higher load levels, shorter on-grid time, and larger capacity ranges, which leads to their flexible regions becoming smaller and slender. The flexibility provided by taxis and rental cars is mainly concentrated in the periods from 10:00 to 14:00 and from 18:00 to 22:00. The schedulable capacity ranges from 10 MWh to 25 MWh, but the load level of rental cars is higher. Thus, they are suitable for participation in energy-only markets.

The official cars and private cars are similar, and the charging load level is low, but there is no large flexible area during the period 18:00-22:00, which is in line with the characteristics of official cars not going home to charge. The bus is a special vehicle with a fixed route, low plug-in battery capacity, and a large charging load. The flexibility of the bus is very low.

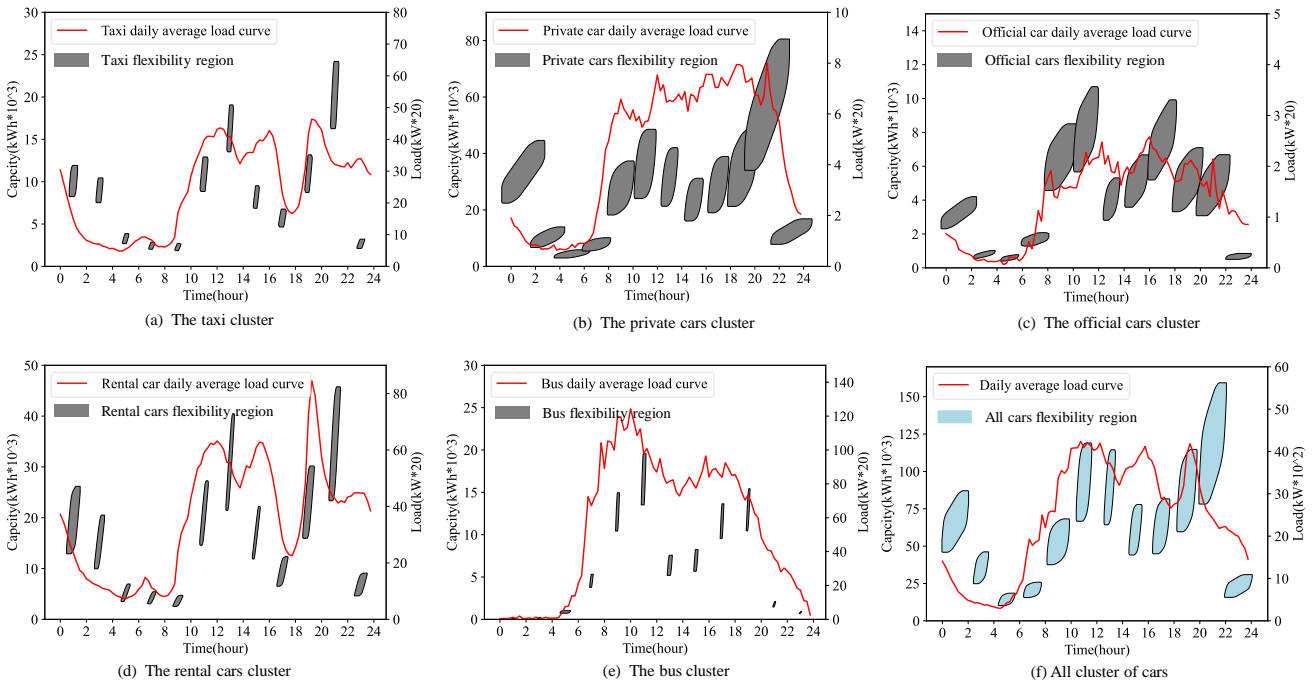


Fig. 10 Aggregation results of the flexible region of each EV user cluster

### 6.3 Analysis of influencing factors

The flexibility of electric vehicles is influenced by a variety of factors, such as the number of electric vehicles and traffic conditions, and this section analyzes these factors in detail. The number of flexible regions from each EV cluster before aggregation is shown in Fig.11; the number of flexible regions is positively correlated with the number of vehicles. Fig. 10 (f) illustrates the flexible region aggregation result for all EV users.

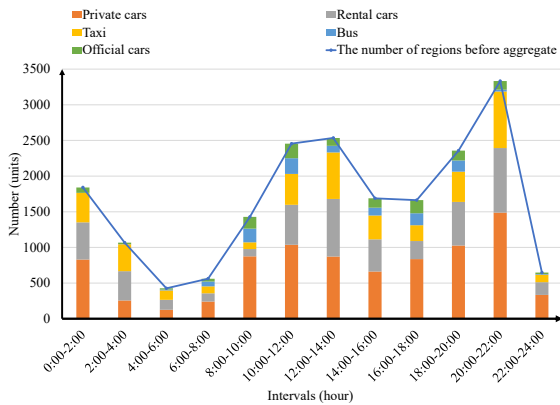


Fig. 11 The user class composition of flexible region in each interval

The flexibility of all EV users is predominantly attributed to private cars, which is a consequence of the larger number of private cars in the overall vehicle fleet. While rental vehicles and taxis constitute a smaller proportion of the overall vehicle fleet compared to private cars, their higher mileage potential, and higher charging power, the flexibility contributed cannot be

ignored. In conjunction with Fig.11, the specific analysis is as follows: private cars account for a relatively high period, and the flexible region is large, such as 0:00-2:00, 18:00-22:00. In these periods, the flexible region of EVs is significantly affected by private cars with low charging power and long on-grid time. EVs are suited to the capacity market during these periods. Although the quantity of rental vehicles and taxis is not comparable to that of private cars, they exhibit higher charging frequency and consistently occupy a significant proportion within the flexible region. When the rental cars and taxi occupy a relatively high period, the flexible region of EVs will become smaller and slender, such as 10:00-14:00 two periods, which is due to the high charging power of taxis and rental cars, and the short on-grid time. EVs are suitable for the energy-only market during these periods.

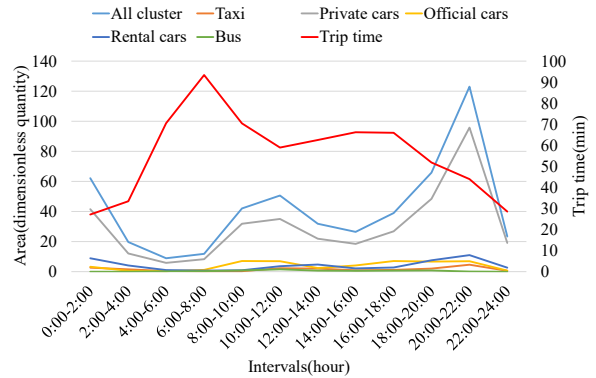


Fig. 12 The area of EV flexible region and the trip time in Nanjing

The area of EV flexible region and the trip time in Nanjing during each interval are presented in Fig.12. A larger area indicates greater flexibility. Longer trip durations suggest less favorable road conditions.

It can be seen from the changes of EV flexible region area and trip time, the flexibility of the EV cluster is inversely proportional to road conditions, with better road conditions resulting in greater flexibility. During the congested morning peak hours, the flexibility of the EV cluster is significantly reduced compared with the evening peak hours, and this congestion leads to increased power consumption. In conjunction with Fig.10, between 8:00-10:00 after the morning peak, the capacity adjustment range for the EV cluster is limited to 25 MWh-60 MWh, indicating a

lower plug-in capacity during this period. Conversely, between 18:00-22:00 after the evening peak when road conditions are improved, the EV cluster exhibits a larger flexible region and higher upper and lower limits, indicating a higher plug-in capacity at that time.

#### 6.4 District flexibility analysis

Owing to the temporal and spatial nature of EV charging and based on the analysis of the flexibility of EV clusters in the preceding section, the flexibility of the charging area can be deliberated, which can offer a preliminary conclusion for considering the flexibility of EVs in the development of urban power systems.

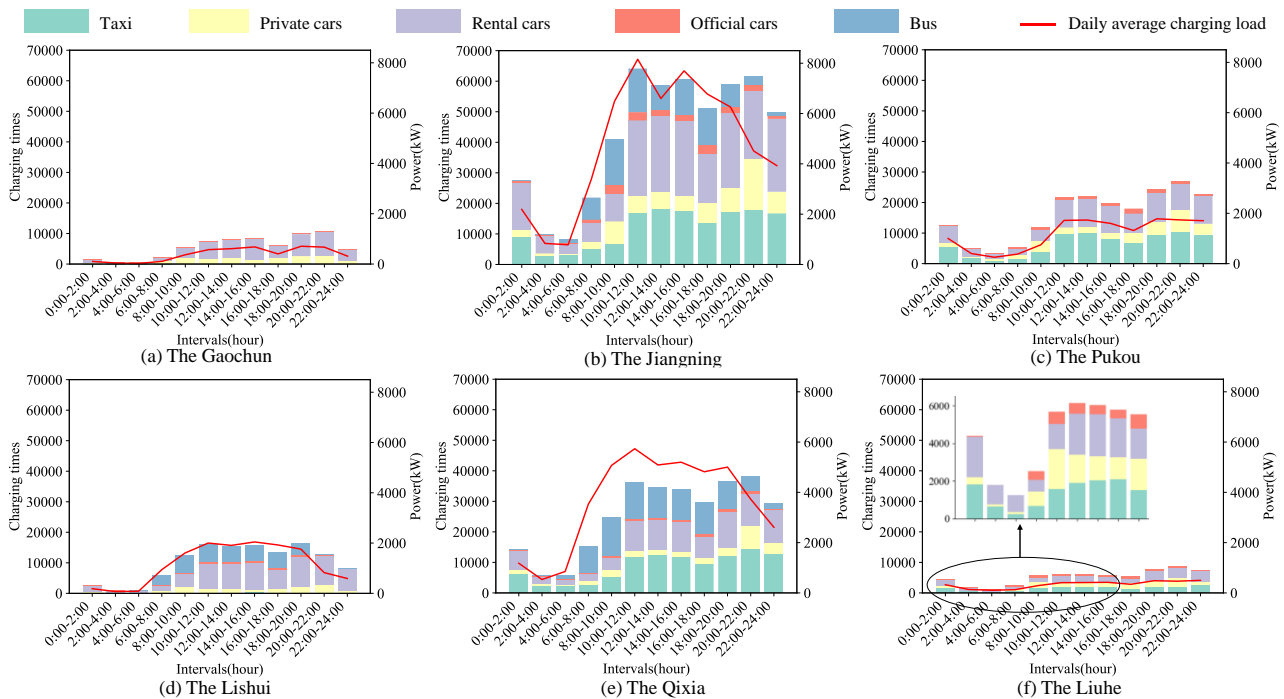


Fig. 13 Distribution of charging vehicles and daily average charging load by districts

The distribution of charging vehicles and the daily average charging load curve in the six districts of Nanjing are shown in Fig.13. An analysis of charging frequency reveals that Jiangning District exhibits the highest frequency of charging activities, potentially indicating enhanced operational flexibility within its electric vehicle fleet and can participate in vehicle-to-grid interaction to effectively address issues such as grid overload. Conversely, Liuhe District exhibits the lowest charging frequency among the districts under consideration. The flexibility of EVs in the district is limited, and the base load is minimal. Consequently, it is necessary to collaborate with other load-side resources to address the power grid challenges in the district.

The time distribution of charging activity shows that the charging activity in each district is relatively

minimal in 0:00-8:00. The EV charging behavior in Jiangning, Qixia, and Pukou districts exhibited bimodal characteristics, albeit with temporal variations in peak occurrences, indicating that these districts experience EV flexibility peaks during distinct intervals. Gaochun and Liuhe districts exhibit similar EV charging patterns across various time intervals. In contrast, Lishui District demonstrates a unimodal peak in EV charging behavior, with negligible charging activity observed in 00:00-06:00. This observation suggests that EVs in this district have limited capacity to provide flexibility during the early morning hours. In addition to Jiangning District, the charging frequency in the remaining districts in 18:00-24:00 is marginally higher than that in 12:00-16:00, suggesting that the concentration of workplaces in Jiangning District is substantial, resulting in a significant number of users charging at midday. This phenomenon also

leads to variability in flexibility even within the same time interval, necessitating that the power grid comprehensively consider both temporal and spatial characteristics to formulate appropriate measures.

Regarding the vehicle composition in each district, Gaochun District exhibits distinct characteristics, primarily comprising rental and private vehicles. Based on the aforementioned analysis of EV clusters, this district demonstrates potential to offer flexibility in both the capacity market and the energy-only market. The vehicular composition of Jiangning District exhibits considerable diversity, demonstrating a notable capacity for participation in both capacity and energy-only markets. The electric vehicles charging in Lishui District predominantly comprise buses and rental cars. This composition is attributable to the area's distance from the city center, its low urbanization rate, and the scarcity of private cars and taxis, factors which render it more conducive to participation in the energy-only market. The vehicular composition in Pukou, Qixia, and Liuhe exhibits similarities. However, a notable distinction lies in the presence of buses in Qixia, which potentially possess greater capacity for participation in the energy-only market. The private vehicles in the Liuhe District demonstrate a charging peak 8:00-10:00. This phenomenon is attributable to the presence of extensive industrial parks in the district, where private car users initiate charging upon arrival at their workplace.

Several factors contribute to this phenomenon. Based on the charging frequency in each district and the analysis results of EV cluster flexibility mentioned above, this study categorizes EV flexibility in each district into six levels. Additionally, data such as GDP, population, and area are collected for each district to examine their relationship with EV flexibility in that particular area. This is illustrated in Tab.2.

The correlation analysis of this data set reveals that the flexibility of each district exhibits a strong positive correlation with GDP and population, with correlation coefficients of 0.82 and 0.77, respectively. However, there is no significant correlation between flexibility and area (correlation coefficient = 0.06). These findings suggest that the flexibility of EVs in a district is primarily influenced by its economic strength and population size rather than its area. Consequently, these results offer valuable insights for potential applications leveraging EV flexibility in urban areas, emphasizing the importance of prioritizing regions with higher GDP and population. (It is noteworthy that despite Lishui's higher GDP and population, its electric vehicle (EV) charging frequency and vehicle type diversity are marginally inferior to those of Pukou District, leading to the conclusion that Lishui exhibits less flexibility than Pukou.).

Tab. 2 District data sets and flexibility rankings

District	GDP (billion CNY)	Population	Area(km <sup>2</sup> )	Flexibility rank
Jiangning	3056.19	1985,200	1563.33	6
Qixia	1783.56	1012,700	395.44	5
Pukou	529.95	414,500	910.49	4
Lishui	1061.76	513,000	1063.67	3
Liuhe	613.54	640,800	1471	2
Gaochun	59.035	440,000	790.22	1

## 6.5 Comparative analysis of proposed method

In order to better realize the aggregation of the EV flexible region, the original generator is improved so that the approximation model is more suitable for the EV flexible region. Tab.3 shows the average similarity  $\overline{\Delta_z}$  that the approximate model can achieve before and after improve, and the average similarity is improved from 0.305 to 0.871, which proves that the modified generator is effective.

Tab.4 shows the time of EV flexible region aggregation for various EVs. The total time for the 20160 EV flexible region aggregation is 41.96 seconds. As the number of EV flexible regions decreases, the calculation time also decreases. The proposed method can complete the aggregation for different types of vehicles, and the calculation time is fast.

Tab. 3 Average similarity of approximate model

Average similarity	Original generators	Proposed generators
$\overline{\Delta_z}$	0.305	0.871

Tab. 4 The aggregation time of each EVs

EVs	Bus	Official cars	Taxi	Rental cars	Private cars	Total
Number of regions	1059	1231	4075	5060	8735	20160
Time(s)	2.45	2.85	9.65	11.35	20.36	41.96

## 7 Conclusion and future study

A method to characterize the flexibility of EVs based on real user behavior data is proposed. Based on the clustering algorithm, the charging habits of the users are mined by clustering the plug-in time for each user. The flexibility potential is quantified by establishing an evaluation index for each cluster of each user. Then, based on the indexes for each cluster of each user, the flexible region of a single EV user is constructed, and the flexibility of EV users in the 24-hour period is analyzed. Finally, the flexible region of EV users is aggregated by using the zonotope

approximation and the Minkowski sum, and the flexible region of all EV users is obtained.

A real dataset is used in this study. The characteristics of different types of flexible regions, flexibility of different EV user clusters in each period, and influence of user types and road conditions on EVs flexibility are analyzed. The EV flexibility of each district is also analyzed, which provides an a priori reference for cities to utilize EV flexibility. Simultaneously, the similarity is improved by 0.566 when approximating the EV flexible region by modifying the generator. The results of these analyses reflect the flexibility of the EVs. The upward-downward adjustment ability of the EVs flexibility under different time periods is analyzed, which provides a reference for EVA dispatching EVs to participate in the flexibility adjustment of the power grid. The EVA can be scheduled directly according to the shape characteristics and boundary of the EVs flexibility region.

The proposed method needs to be improved. The following is a summary of future research.

1) The impact of network facility supply on the flexibility characterization of users is not discussed in the manuscript. However, with the development of smart grids, the cyber threat brought about by the smart grid infrastructure is becoming increasingly prominent. Data leakage, malware attacks, denial of service attacks, etc., may undermine the stability of the power grid, resulting in the interruption of charging services and damage to facilities, thus affecting the flexibility of EV users. Therefore, it is necessary to study this further in the future.

2) The EV flexibility index uses the average value to represent the long-term behavior habits of users. In the future, the probability distribution model will be used to characterize the charging and discharging habits of EV users, and an EV flexibility region model including the probability distribution will be proposed.

3) An EV flexible region based on the dispatching capacity is constructed. Further research should be conducted on dispatching power regions.

## 8 ACKNOWLEDGEMENT

This work was financially funded by Chunhui Project Foundation of the Education Department of China (Grant/Award Numbers: HZKY20220265).

## References:

- [1] Ma J, Silva V, Belhomme R, Kirschen DS, Ochoa LF. Evaluating and Planning Flexibility in Sustainable Power Systems. *IEEE Transactions on Sustainable Energy* 2013;4:200-209. <https://doi.org/10.1109/TSTE.2012.2212471>.
- [2] International Energy Agency, Global EV Outlook

- 2024: Catching up with Climate Ambitions. in *Global EV Outlook*. OECD, 2024. <https://doi.org/10.1787/cbe724e8-en>.
- [3] Yao Y, Zhao R, Li C, Yan Z, Xie K. Control Strategy of Electric Vehicles Oriented to Power System Flexibility. *Transactions of China Electrotechnical Society* 2022;37:2813-2824. <https://doi.org/10.19595/j.cnki.1000-6753.tces.210515>
- [4] Zade M, Incedag Y, El-Baz W, Tzscheuschler P, Wagner U. Prosumer Integration in Flexibility Markets: A Bid Development and Pricing Model. in *2018 2nd IEEE Conference on Energy Internet and Energy System Integration (EI2)* 2018;1-9. <https://doi.org/10.1109/EI2.2018.8582022>.
- [5] Zhang B, Kezunovic M. Impact on Power System Flexibility by Electric Vehicle Participation in Ramp Market. *IEEE Trans. Smart Grid* 2016;7:1285-1294. <https://doi.org/10.1109/TSG.2015.2437911>.
- [6] Gunkel PA, Bergaentzlé C, Græsted Jensen I, Scheller F. From passive to active: Flexibility from electric vehicles in the context of transmission system development. *Applied Energy* 2020;277:115526. <https://doi.org/10.1016/j.apenergy.2020.115526>.
- [7] Deng R, Xiang Y, Huo D, Liu Y, Huang Y, Huang C, et al. Exploring flexibility of electric vehicle aggregators as energy reserve. *Electric Power Systems Research* 2020;184:106305. <https://doi.org/10.1016/j.epsr.2020.106305>.
- [8] Leippi A, Fleschutz M, Davis K, et al. Optimizing electric vehicle fleet integration in industrial demand response: Maximizing vehicle-to-grid benefits while compensating vehicle owners for battery degradation. *Applied Energy*, 2024, 374. <https://doi.org/10.1016/j.apenergy.2024.123995>.
- [9] Pla B, Bares P, Aronis AN, et al. Leveraging battery electric vehicle energy storage potential for home energy saving by model predictive control with backward induction. *Applied energy*, 2024;372. <https://doi.org/10.1016/j.apenergy.2024.123800>.
- [10] Arnold F, Lilienkamp A, Namockel N. Diffusion of electric vehicles and their flexibility potential for smoothing residual demand — A spatio-temporal analysis for Germany. *Energy*, 2024, 308. <https://doi.org/10.1016/j.energy.2024.132619>.
- [11] Zhang H, Hu Z, Xu Z, Song Y. Evaluation of Achievable Vehicle-to-Grid Capacity Using Aggregate PEV Model. *IEEE Trans. Power Syst* 2017;32:784-794. <https://doi.org/10.1109/TPWRS.2016.2561296>.
- [12] Wang L, Kwon J, Schulz N, Zhou Z. Evaluation of Aggregated EV Flexibility With TSO-DSO Coordination. *IEEE Trans. Sustain. Energy* 2022; 13:2304-2315. <https://doi.org/10.1109/TSTE.2022.3190199>.

- [13] Mills G, MacGill I. Assessing Electric Vehicle storage, flexibility, and Distributed Energy Resource potential. *Journal of Energy Storage* 2018;17:357–366. <https://doi.org/10.1016/j.est.2018.01.016>.
- [14] Guthoff F, Klempp N, Hufendiek K. Quantification of the Flexibility Potential through Smart Charging of Battery Electric Vehicles and the Effects on the Future Electricity Supply System in Germany. *Energies* 2021;14:2383. <https://doi.org/10.3390/en14092383>.
- [15] Yu Z, Lu F, Zou Y, Yang X. Quantifying the real-time energy flexibility of commuter plug-in electric vehicles in an office building considering photovoltaic and load uncertainty. *Applied Energy* 2022;321:119365. <https://doi.org/10.1016/j.apenergy.2022.119365>
- [16] Zhang J, Che L, Wan X, Shahidehpour M. Distributed Hierarchical Coordination of Networked Charging Stations Based on Peer-to-Peer Trading and EV Charging Flexibility Quantification. *IEEE Trans. Power Syst.* 2022;37:2961–2975. <https://doi.org/10.1109/TPWRS.2021.3123351>.
- [17] Diaz-Londono C, Colangelo L, Ruiz F, Patino D, Novara C, Chicco G. Optimal Strategy to Exploit the Flexibility of an Electric Vehicle Charging Station. *Energies* 2019;12:3834. <https://doi.org/10.3390/en12203834>.
- [18] Zade M, You Z, Kumaran Nalini B, Tzscheuschler P, Wagner U. Quantifying the Flexibility of Electric Vehicles in Germany and California — A Case Study. *Energies* 2020;13:5617. <https://doi.org/10.3390/en13215617>.
- [19] Munshi AA, Mohamed YAI. Extracting and Defining Flexibility of Residential Electrical Vehicle Charging Loads. *IEEE Trans. Ind. Inf.* 2018;14:448–461. <https://doi.org/10.1109/TII.2017.2724559>.
- [20] Develder C, Sadeghianpourhamami N, Strobbe M, Refa N, Quantifying flexibility in EV charging as DR potential: Analysis of two real-world data sets. in *2016 IEEE International Conference on Smart Grid Communications*; 2016. p. 600–605. <https://doi.org/10.1109/SmartGridComm.2016.7778827>.
- [21] Ding S, Xu C, Rao Y, Song Z, Yang W, Chen Z, et al. A Time-Varying Potential Evaluation Method for Electric Vehicle Group Demand Response Driven by Small Sample Data. *Sustainability* 2022;14:5281. <https://doi.org/10.3390/su14095281>.
- [22] Sadeghianpourhamami N, Refa N, Strobbe M, et al. Quantitative analysis of electric vehicle flexibility: A data-driven approach. *International Journal of Electrical Power & Energy Systems* 2018;95:451–462. <https://doi.org/10.1016/j.ijepes.2017.09.007>.
- [23] Yang Z, Peng S, Liao Q, Liu D, Xu Y, Zhang L, et al. Ancillary Services Provided by Electric Vehicles for Building Integrated Energy System. *Power System Technology* 2017;41:2831–2843. <https://doi.org/10.13335/j.1000-3673.pst.2017.0788>
- [24] Ortega-Vazquez MA, Bouffard F, Silva V. Electric Vehicle Aggregator/System Operator Coordination for Charging Scheduling and Services Procurement. *IEEE Trans. Power Syst* 2013;28:1806–1815. <https://doi.org/10.1109/TPWRS.2012.2221750>.
- [25] Hu J, Ma Wen, Xue Y, Yao L, Xie D. Quantification of Reserve Capacity Provided by Electric Vehicle Aggregator Based on Framework of Cyber-Physical-Social System in Energy. *Automation of Electric Power System* 2022;46:46–54.
- [26] Deng Z, Feng X, Wang S, Li H, Liu J. Comprehensive Optimal Scheduling of VPP with EV Cluster Participating in Main and Auxiliary Joint Markets. *Proceedings of the CSU-EPSC* 2023;35:83–93. <https://doi.org/10.19635/j.cnki.csu-epsa.000999>
- [27] Zhu X, Sun Y, Yang B, Yang J, Wu F, Li G, et al. Calculation method of EV cluster’s schedulable potential capacity considering uncertainties and bounded rational energy consumption behaviors. *Electric Power Automation Equipment* 2022;42:245–254. <https://doi.org/10.16081/j.epae.202209010>
- [28] Jian J, Zhang M, Xu Y, Tang W, He S. An Analytical Polytope Approximation Aggregation of Electric Vehicles Considering Uncertainty for the Day-Ahead Distribution Network Dispatching. *IEEE Trans. Sustain. Energy* 2024;15:160–172. <https://doi.org/10.1109/TSTE.2023.3275566>.
- [29] Zhao W, Huang H, Zhu J, Zhou B, Chen J, Luo S. Flexible Resource Cluster Response Based on Inner Approximate and Constraint Space Integration. *Power System Technology* 2023;47:2621–2632. <https://doi.org/10.13335/j.1000-3673.pst.2022.1935>.
- [30] Zhou H, Liu Y, Chen Y, Wang Z, Qu S, He K, et al. Demand Side Feasible Region Aggregation Considering Flexibility Revenue. *Electric Power* 2022;55:56–63.
- [31] Muller FL, Szabo J, Sundstrom O, Lygeros J. Aggregation and Disaggregation of Energetic Flexibility From Distributed Energy Resources. *IEEE Trans. Smart Grid* 2019;10:1205–1214. <https://doi.org/10.1109/TSTE.2023.327556610.1109/TSG.2017.2761439>.
- [32] Muller FL, Sundstrom O, Szabo J, Lygeros J. Aggregation of energetic flexibility using zonotopes. in *2015 54th IEEE Conference on Decision and Control*; 2015. p. 6564–6569.

<https://doi.org/10.1109/CDC.2015.7403253>.

- [33] Boyd S , Vandenberghe L .Convex Optimization.  
Cambridge university press,2004;p.31-34